ORIGINAL ARTICLE

Assessment of flood risk by using geospatial techniques in Wabi Shebele River Sub-basin, West Hararghe Zone, southeastern Ethiopia

Biratu Bobo Merga[1] · Feye Lama Mamo[2] · Mitiku Badasa Moisa[3] · Firdisa Sadeta Tiye[4] · Dessalen Obsi Gemeda[5]

Abstract

Floods are produced as a result of several factors such as human-induced land-use changes, topographic conditions, and climate change. This study aimed to assess flood risk using geographic information system-based multi-criteria evaluation techniques in the Wabi Shebele River Sub-basin. Six parameters, namely, soil type, slope, land use and land cover, proximity to rivers, rainfall, and elevation, were used. The eigenvector of weight for each factor was computed in IDRISI Selva 17.0. Results show that the study area was subjected to a very high 527.31 km^2 (9.42%), high 2133.66 km^2 (38.12%), moderate 1906.44 km^2 (34.06%), low 847.35 km^2 (15.14%), and a very low 182.54 km^2 (3.26%) flood risk, respectively. Results reveal that the Wabi Shebele River Sub-basin is highly vulnerable to flooding. This study assists policymakers with regard to land-use planning. To reduce the effects of flood risk, integrated watershed management must be implemented in the study area.

Keywords Flood risk · Shebele River Sub-basin · MCE · AHP

Introduction

Floods are one of the worst natural disasters that can happen anywhere in the world, causing significant damage and having a significant socioeconomic impact on various sectors (Sun et al. 2020; Zhao et al. 2022; Yang et al. 2023; Wu et al. 2023). An increase in the frequency of flooding is one of the effects of climate change (Xu et al. 2022; Gao et al. 2023). In terms of both quantity and losses, floods represent 34 and 40% of all-natural disasters worldwide, respectively (Lyu et al. 2019; Xie et al. 2021; Yuan et al. 2023). There are

significant varieties that influence the environment such as elevation differences and surface coverage, socioeconomic factors (e.g., population and built-up areas), and disaster-prone bodies (e.g., transportation facilities in different locations) (Zhang and Chen 2019; Huang et al. 2021; Zhou et al. 2021a).

It is important to manage and control floods that affect the agricultural economy, which is the mainstay of densely populated areas (Miller and Shaw 2015; Zhou et al. 2021b; Yin et al. 2023d; Ma et al. 2023). This is technically impossible without the accurate mapping of flood hazards and risks.

✉ Biratu Bobo Merga
  bira2bobo@gmail.com

  Feye Lama Mamo
  feyera19@yahoo.com

  Mitiku Badasa Moisa
  mitikubadasa10@gmail.com

  Firdisa Sadeta Tiye
  firdisadeta@gmail.com

  Dessalen Obsi Gemeda
  dasoobsi@gmail.com

[1] Department of Geographic Information Science, Institute of Land Administration, Oda Bultum University, Chiro, Ethiopia

[2] Department of Hydraulics Engineering, Institute of Technology, Oda Bultum University, Chiro, Ethiopia

[3] Department of Earth Sciences, College of Natural and Computational Sciences, Wollega University Nekemte Campus, Nekemte, Ethiopia

[4] Department of Geography and Environmental Studies, College of Social Science and Humanities, Wollega University, Gimbi Campus, Gimbi, Ethiopia

[5] Department of Natural Resource Management, College of Agriculture and Veterinary Medicine, Jimma University, Jimma, Ethiopia

Rapid population growth is rapidly accelerating, increasing pressure on farmland, which has increased the change in land use and land cover (LULC) that could lead to flooding (Li et al. 2021; Moisa and Gemeda 2021; Negash et al. 2021; Moisa et al. 2022; Merga et al. 2022).

In Ethiopia, the most frequently flooded areas include the Awash River Basin, the Wabi Shebelle River Basin, and the Baro-Akobo Basin. The Wabi Shebelle River Basin is one of the Ethiopia's major river basins and is prone to flooding (Wondim 2016). Flooding has forced thousands of people to flee their homes and caused massive economic losses and environmental damage (Getahun and Gebre 2015).

The Wabi Shebele River Sub-basin is one of the major areas being affected by flooding. The majority of flood damage in the study area is seemingly caused by a few days of intense rainfall with an average intensity of 10–200 mm/hr and a total quantity of precipitation of 100 mm. Flood events have occurred frequently in the basin, manifesting as flash floods in the lowland areas, as shown by the state of the river banks and sheet erosion (Ethiopian Ministry of Water Resource 2004).

Previously, several studies have been conducted on the significant impacts of flooding on most parts of Ethiopia. According to Abaya et al. (2009) studies, flooding frequency and magnitude have significantly increased in the Gambela region due to *a* lack of flood-specific policy, little risk assessment, and weak institutional capacity, which directly result in death, injuries, and disease outbreaks in the local communities of the region. Flooding from Lake Tana's surface water discharge displaced the local community from their land each year (Tarekegn et al. 2010). The study done by Getahun and Gebre (2015) indicate*s* that the upstream and middle are more vulnerable to flood risk than the downstream parts of the Fetam Watershed of the Upper Abbay Basin of Ethiopia.

However, most previous scholars did not emphasize the identification of flood risk-prone areas, which enhance*s* prioritization for future conservation practices in monitoring the significant impacts of flood risk on natural resource*s* and human life. Identifying and mapping the spatial distribution of the flood-prone zone enhance*s* land-use planners and natural resource manager's ability to apply risk management strategies at the right time. Geographic Information System*s* (GIS) and remote sensing, along with multi-criteria evaluation (MCE) techniques, play a great role in assessing flood risk. Therefore, the present study aimed to fill the existing research gap by assessing flood risk-prone areas using geospatial techniques and the analytical hierarchy process (AHP) in the Wabi Shebele River Sub-basin of southestern Ethiopia.

Materials and methods

Description of the study area

The Wabi Shebele River Sub-basin (current study area) is located in the West Hararghe Zone of Oromia Regional State. Geographically, it is situated between latitude and longitude of 8°0′0″ to 8°48′0″ N and 40°24′0″ to 41°12′0″ E. The study area covers about 5596.34 km² with an elevation ranging from 703 to 2988 m above mean sea level (Fig. 1).

The major rainy season in the study area lasts from July to September, and the minor wet season from February to April. The annual average rainfall varies between 760 and 1200 mm. The wettest months are June, July, and August, while the driest months are May, June, March, September, and October. The local rain is heavy and showery, with low volumes and a sluggish onset. Typically warm winter weather prevails. Summer and winter average temperatures are 25 °C and 30 °C, respectively (Zonal Irrigation Development Authority 2014).

Data sources and descriptions

Several data source*s* were used to achieve the stated objective in the study area. The geographic area of the study area is located between 67 paths and 54 raw reference systems. Landsat 8 operational land imagery (OLI) and thermal infrared sensor (TIRS) of cloud free were downloaded from the USGS website for the year 2022 with a spatial resolution of 30 m for land-use and land-cover classification. The National Metrological Agency also used the five stations in the study area to obtain rainfall data for the year 2022: *Bedesa, Gelemso, Abomsa, Sheki-Husen, and Seru* stations. In addition, soil type data were collected from the Ministry of Water and Irrigation Engineering, while Shuttle Radar Topographic Mission (SRTM) was downloaded from the USGS website to calculate the slope of the study area. Finally, GIS data from 2018 were used to calculate the equidistance of the water source to the study area (Table 1; Fig. 2).

Software package used

ArcGIS 10.3 software was used to analyze and visualize the geospatial data of the study area. In addition, IDRES Selva 17 software was applied for parameter pairwise comparison, whereas ERDAS 2015 software was used for image preprocessing, layer staking, and false color band combination during image classification. Similarly,
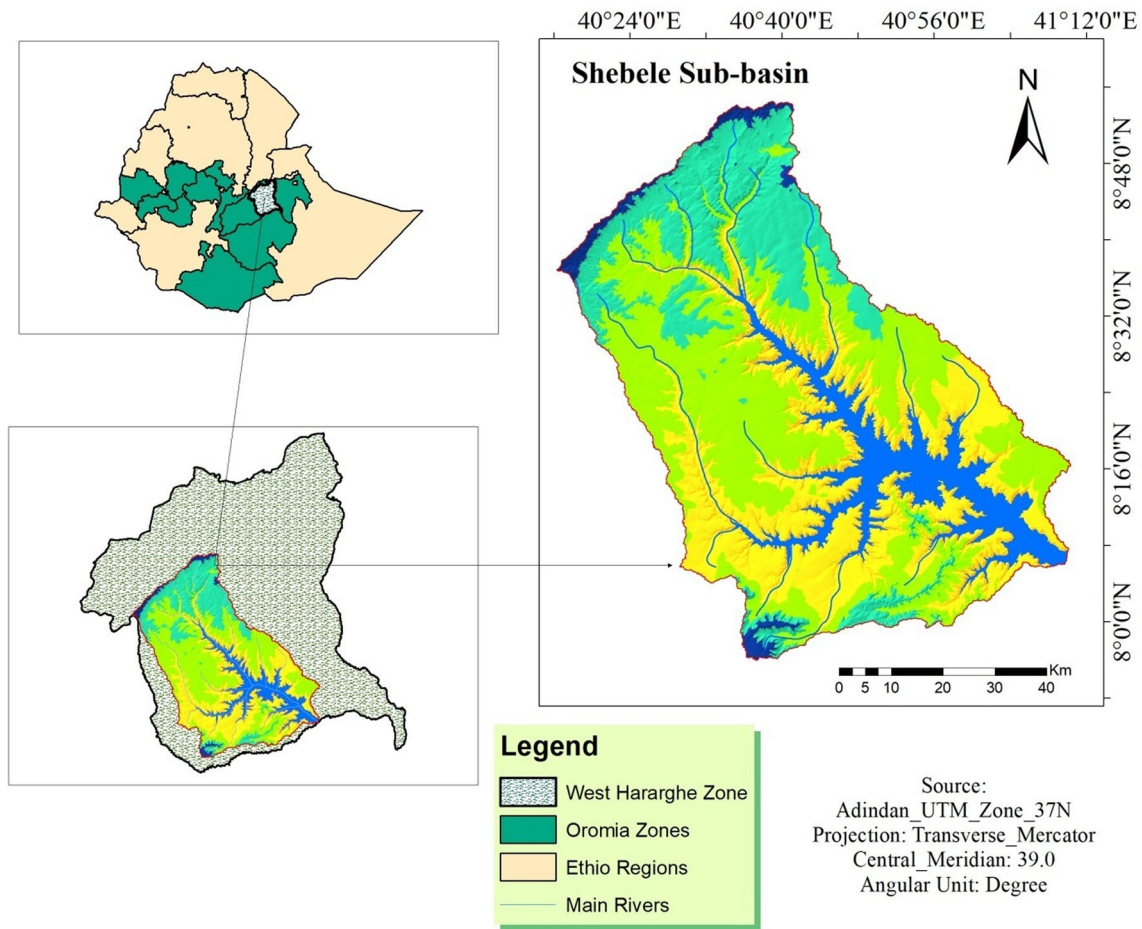
40°24'0"E   40°40'0"E   40°56'0"E   41°12'0"E

Shebele Sub-basin

N

8°48'0"N
8°32'0"N
8°16'0"N
8°00'0"N

Km
0 5 10   20   30   40

Legend
- West Hararghe Zone
- Oromia Zones
- Ethio Regions
- Main Rivers

Source:
Adindan_UTM_Zone_37N
Projection: Transverse_Mercator
Central_Meridian: 39.0
Angular Unit: Degree

Fig. 1 Location map of the study area

Table 1 Data sources and description

Data	Data type	Resolution (m)	Sources
Landsat image	Land use and land cover	30	USGS
Climate data	Rainfall	30	NMA
SRTM data	Slope, elevation	30	USGS
Soil data	Soil type	30	MoWIE
Infrastructure data	Water source	30	EMA

ArcSWAT software was also used to generate the stream network and boundary of the study area.

Data analysis

Rasterization was performed for appropriate parameter weighted overlay analysis under GIS environments. The *w*eighted importance value of each parameter was calculated in IDRISI *S*elva 17 software by using the artificial hierarchy process (AHP) method for pairwise comparison based on their percent of influence in determining the status of flood risk in the study area. During pairwise comparisons, the relative importance value for each parameter in identifying flood risk-prone areas was decided by an expert's opinion based on Saaty's 9-point weighing scale. The pairwise comparison matrix was made by assigning a relative importance value for each parameter and normalizing the eigenvector of the factors by their cumulative total (Wind & Saaty 1980).

Parameters used for flood risk assessment

Soil types

Soil types may be considered one of the critical factors in defining flood-prone areas. It has a significant impact on the rate of precipitated water infiltration and water-holding capacity. Four different major soil types existed in the Wabi Shebele River Sub-basin. These are Calcic Regosols, Eutric Cambisols, Haplic Xerosols, and Haplic Yermosols. According to Wondim (2016), infiltration has a significant impact
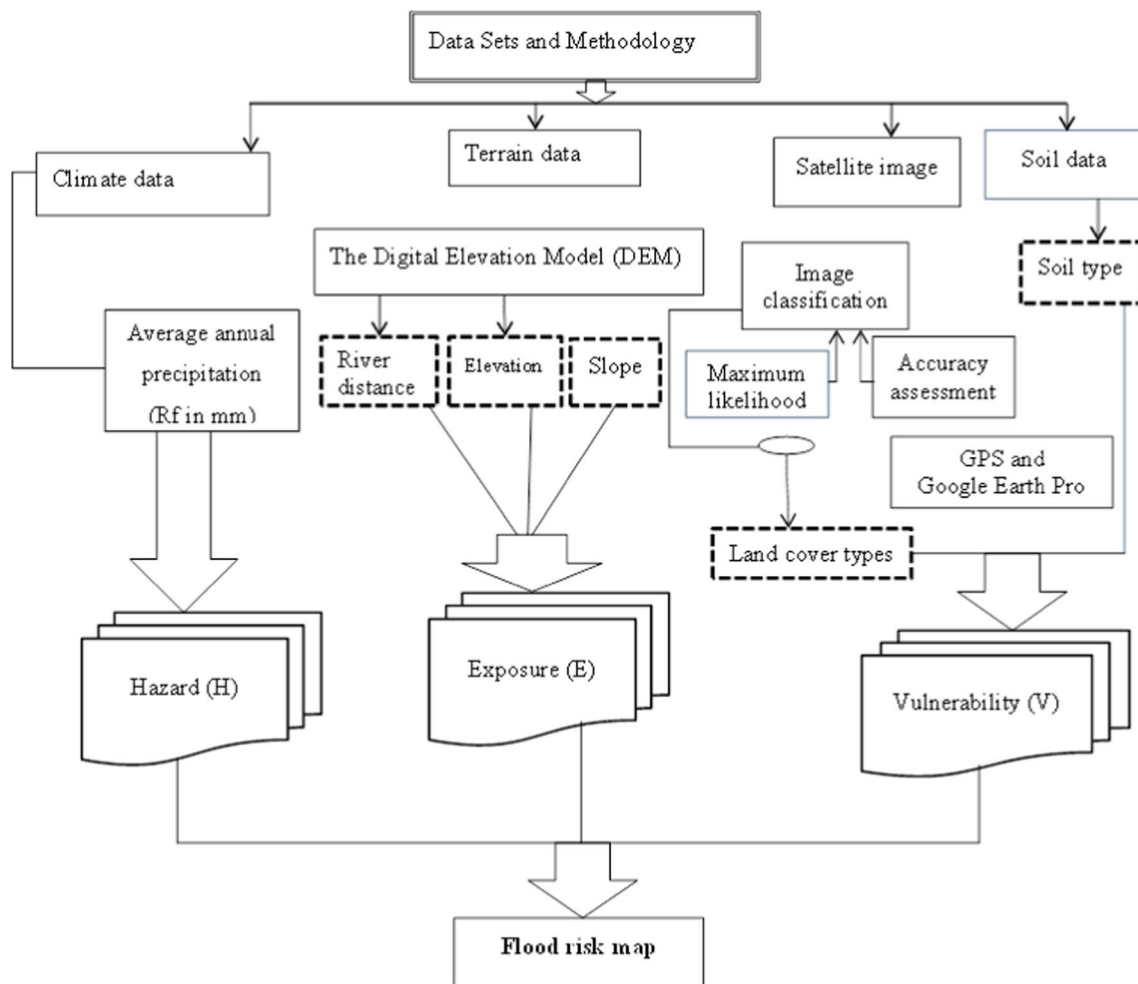
Fig. 2 Methodological flowchart

on the availability and quantity of surface runoff produced by the rainfall runoff process. As a result, clay soil infiltrates at a much lower rate than sandy soil (Hagos et al. 2022).

Slope

The slope of the study area was generated from STRM DEM by degree. According to Hagos et al. (2022), slope was classified into 0°–2°, 2.1°–5°, 5.1°–15°, 15.1°–35°, > 35.1° and very high, high, moderate, low, and very low, respectively. Steep slopes tend to reduce the amount of infiltration of water into the ground; the water can flow quickly down to rivers as overland flows. In addition, steep slopes also cause more through flow within the soil. In reality, due to the fact that water accumulates gradually inside the process of moving alongside the slope from high to low and flood typically nearest happens within the lower place, so the slope length is an element that affects both floods as well as the opportunity of flooding.

LULC analysis

LULC in the sub-basin plays an important role in flooding by delaying or accelerating surface flow. These LULC types of the study area were classified from Landsat OLI/ TIRS of 2022 by using supervised classification with maximum likelihood. As *a* result, the LULC types of the Wabi Shebele Sub-basin were classified into forest, farmland, grassland, shrubland, and settlement. Land use, population density, and population growth in the basin are all considered factors that contribute to flooding (Kundzewicz and Stoffel 2016; Yin et al. 2023c). Even though the study area is largely covered in forest, flooding has a significant impact on farmland and settlement areas. This demonstrates unequivocally that the flood magnitude is strongly negatively correlated with forest cover and positively correlated with cultivated land (Liu et al. 2017; Zhu et al. 2022).

Distance from river

Proximity to a water source can determine the severity and status of flood risks in the study area. The amount of water generated from rainfall, stream*s*, tributaries, and underground recharge increases the volume of the water and causes surface water discharge in the form of flood*s*. This phenomenon indicates that the area of the study area nearest to the water body was more vulnerable to flood risk than the fairest one (Ullah and Zhang 2020; Yin et al. 2023a).

Rainfall

The status and seasonality of the rainfall are also key determinants for evaluating the impacts of flood risks in the study area. Both rainfall and flood risks possess positive relationship*s* (Li et al. 2022; Yin et al. 2023b). Heavy rainfall conditions result in the occurrence of higher flooding risks on the surface of the study area and vice versa. In addition, rainfall also increases the volume of the water in the water body and increases the severity of surface water flooding in the study area (Assefa 2018).

Elevation

Elevation shows the location of the study area above or below sea level. It can determine the speed of runoff and the status of flood accumulation in the study area. An area with lower elevation was characterized by lower flood risks and higher flood accumulation and vice versa.

Accuracy assessment

Accuracy assessment was also made to evaluate the quality of classification output in this study. Error matrix based on assessment of the overall accuracy, producer's accuracy, user's accuracy, and kappa coefficient was utilized. The main goal of accuracy assessment is to quantitatively assess how efficiently the pixels were tested into the correct land-cover classes (Bhatt 2008). To validate the result with ground truth, field data were collected using handheld global positioning system (GPS), and finally, land-use and land-cover classes were identified and mapped for further analysis. The result of accuracy assessment provides an overall accuracy of the map based on an average of the accuracies for each class in class in the map (Girma et al. 2020; Moisa et al. 2023).

$$OAC = \frac{\Sigma Xij}{N} \times 100 \tag{1}$$

$$Khat = \frac{(Obs - \exp)}{(1 - Exp)} \tag{2}$$

where OAC is over all accuracy, UAC is user accuracy, PAC is producer accuracy, Khat is Kappa statistics, N is total number of samples, Xij is the diagonal values, $Xi+$ is the column total, $X+i$ is row total, r is the number of categories, Obs is accuracy reported in error matrix (overall accuracy), and Exp represents correct classification.

Parameters rating scale for flood risk assessment

The scale variation in all targeted parameters may cause the presence of various flood risks in the study area (Table 2). Estimation of such variation enables land managers to identify flood risk-prone areas and prioritize future conservation.

Analytical hierarchy process

During this study, six ecological parameters, including soil type, slope, LULC, elevation, rainfall, and proximity

Table 2 Scaled and weighted of flood risk and hazard factors

Factor	Weight	Sub-factor	Scale
Elevation (m)	0.2899	0.0 703–1100	Very high
		1.0 1100–1500	High
		2.0 1500–1900	Moderate
		3.0 1900–2400	Low
		4.0 2400–2988	Very low
Slope (degree)	0.1688	5.0–2	Very high
		2.1–5	High
		5.1–5	Moderate
		15.1–35	Low
		> 35.1	Very low
LULC	0.1419	Farmland	Very high
		Settlement	High
		Grassland	Moderate
		Shrubland	Low
		Forest	Very low
Soil type	0.0849	Eutric Cambisols	Very high
		Haplic Xerosols	High
		Calcic Regosols	Moderate
		Haplic Yermosols	Low
Rainfall (mm)	0.1025	> 1160	Very high
		1060–1160	High
		960–1060	Moderate
		860–960	Low
		760–860	Very low
Distance from rivers (m)	0.0849	< 500	Very high
		500–1000	High
		1000–1500	Moderate
		1500–2000	Low
		> 2000	Very low

to a water source, were assigned for accessing flood risk-prone area*s* in the study area. For each of the targeted parameters, weighted value*s* have been calculated by using the analytical hierarchy process (AHP) method and the multi-criteria decision analysis (MCDA) tool based on a 9-point scale (Saaty 2008). The reliability of the parameter weighted value was evaluated based on the relative importance value assigned by exports for each parameter (Table 3).

Pairwise comparison matrix has been performed by using assigned relative importance value of each parameter in EDRIS Selva 17 to evaluate the flood risk vulnerability of the study area (Table 4).

The pairwise comparison acceptability was based on the calculated value of consistency ratio (CR) which must be less than 0.1 (Moisa et al. 2023), and the consistence ratio in the present study was 0.06. The consistency ratio for parameters pairwise comparison was determined as Eq. (3).

$$CR = \frac{CI}{RI} \tag{3}$$

where CI represents consistency index, and RI represents random consistency index.

Consistency index was the measure of how all targeted parameters were interrelated and calculated as Eq. (4).

$$CI = \frac{\lambda \max - n}{n - 1} \tag{4}$$

where n indicates the number of parameters, and λmax refers to the principal eigen value of parameters that can be calculated from multiplication of the total horizontal summation of given intensity importance value and parameters weighted value. The normalized principal eigenvector was obtained from averaging the normalized relative weight of the parameters.

The random consistency index was an assigned constant number based on the number of parameters used in the study (Table 5).

Final flood risk analysis

All criteria map of the parameters were overlaid by using parameters suitability index to calculate flood risk-prone area in the study area. According to Debesa et al. (2020), flood risk area was calculated as Eq. (5).

$$SI = \sum Wi \times Xi \tag{5}$$

where SI is suitability index, *Wi* is weight of factor I, *Xi* is normalized criterion of factors, and $\sum$ is their the summation.

Table 3 The relative importance value

Intensity of parameters importance value	Definition	Description
1	Equal importance	Both parameters have equal influence
3	Somewhat more important	Impact of one parameter slightly favors the other
5	Much more important	Impact of one parameter strongly favors the other
7	Very much important	Impact of one parameter strongly favors the other and the impact demonstrated in practices
9	Absolutely more important	Impact of one parameter has highest possible validity on the other
2, 4, 6, 8	Intermediate importance	When comparison is required

Table 4 Pairwise comparison table

	Dist. river	Elevation	Slope	LU/LC	Rainfall	Soil type	Weight
Dist. river	1	2	2	2	2	2	0.0849
Elevation	1/2	1	2	3	2	2	0.2899
Slope	1/2	1/2	1	2	2	2	0.1688
LULC	1/2	1/3	1/2	1	3	2	0.1419
Rainfall	1/2	1/2	1/2	1/3	1	2	0.1025
Soil type	1/2	1/2	1/2	1/2	1/2	1	0.0849
Σ	3.5	4.83	6.5	8.83	10.5	11	1

Table 5 The random index scale

Intensity importance	1	2	3	4	5	6
Constant number	0.00	0.00	0.58	0.90	1.12	1

Results and discussion

Flood risk factors analysis

To determine flood risk, environmental background conditions such as soil type, slope, elevation, rainfall, and distance from the river, as well as LULC, which are the key flood-producing factors, were analyzed in the study.

Table 6 Soil type

Soil types	Area (km^2)	Area (%)
Eutric Cambisols	620.38	11.64
Calcaric Regosols	516.85	9.24
Haplic Yermosols	595.46	10.64
Haplic Xerosols	3863.65	69.04
Total	5596.34	100.00

Soil types

Soil may be considered one of the critical factors in defining flood-prone areas. It has a significant impact on the rate of precipitated water infiltration and water-holding capacity. The statistical analysis of soil types in the study area shows that a large portion, which accounts for 69.04%, is covered by Haplic Xerosols, followed by Eutric Cambisols, 11.64% (Table 6; Fig. 3). According to Wondim (2016), infiltration has a significant impact on the availability and quantity of surface runoff produced by the rainfall runoff process. As a result, clay soil infiltrates much lower rate than sandy soil (Hagos et al. 2022). Eutric Cambisols were highly vulnerable to flood risk than other soil types in the study area. A northern part of the study area was highly susceptible to flooding in the Wabi Shebele Sub-basin. Ayenew and Kebede (2023) confirmed that Cambisol soil types were highly susceptible to flooding than nitisol soil types.
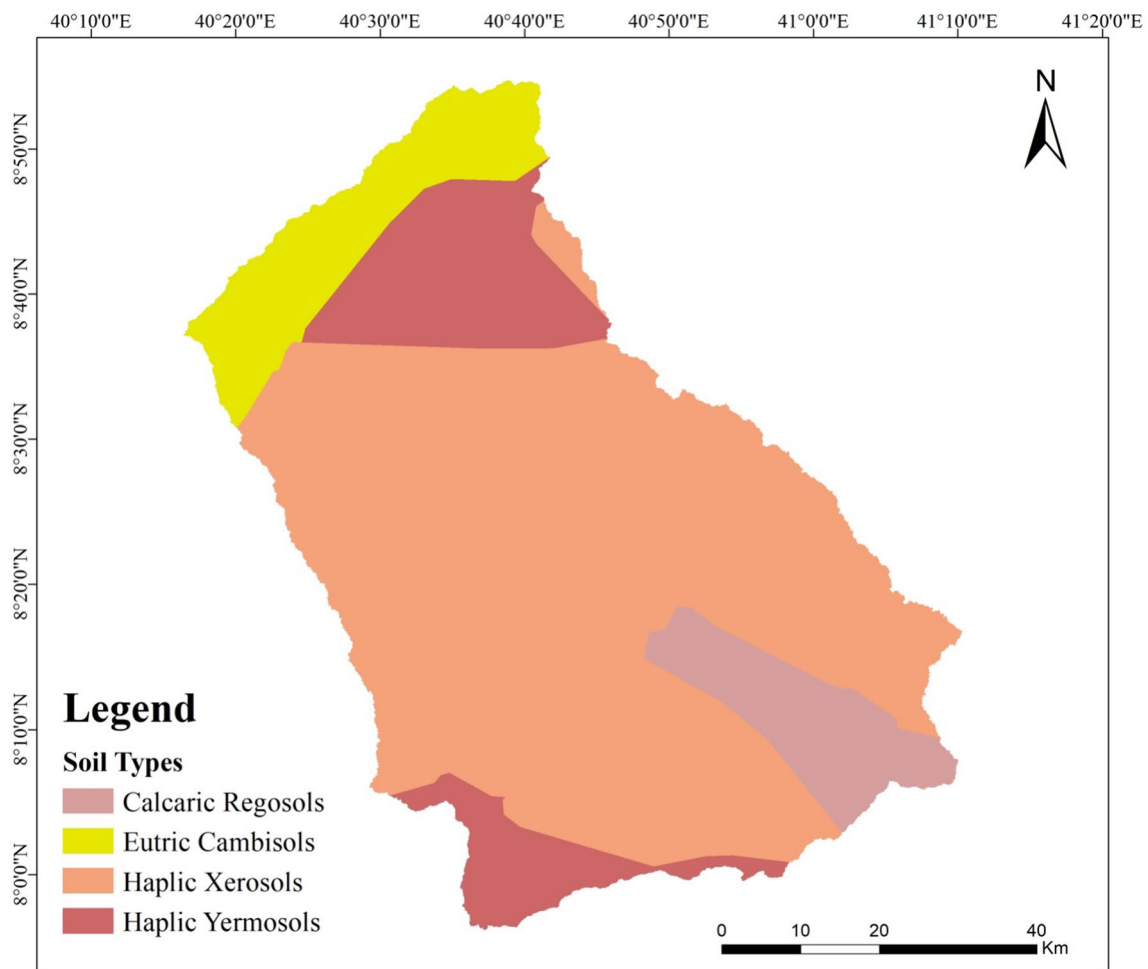

Fig. 3 Soil type of the study area

Slope factor

Steep slopes tend to reduce the amount of infiltration of water into the ground; the water can flow quickly down to rivers as overland flows. In addition, steep slopes also cause more through flow within the soil. In reality, due to the fact that water accumulates gradually inside the process of moving alongside the slope from high to low, and flooding typically happens within the lower place, the slope length

is an element that affects both floods and the opportunity of flooding. The slope in the study area ranges from 0° to 74.24°. A high rating is assigned to low slopes, and a low rating is assigned to high slopes. From the total area of the sub-basin, about 1924.39 km² (34.39%) fall under the slope range between 2.1° and 15°, which was assigned as the high rate for flooding risk (Table 7). Geographically, the central and southeastern parts of the study area were at higher risk for flooding than other directions (Fig. 4). The slope has a great influence on assessing flood risk because it controls the amount of surface runoff (Alemayehu 2007; Hagos et al. 2022; Yin et al. 2023f).

Table 7 Rate of slope for susceptibility to flooding

Slope in (°)	Level	Area (km²)	Area (%)
0.0–2	Very high	794.64	14.20
2.1–5	High	1924.39	34.39
5.1–15	Moderate	1525.04	27.25
15.1–35	Low	1106.70	19.78
> 35.1	Very low	245.57	4.39
Total	–	5596.34	100.00

Land-use and land-cover factor

LULC of the sub-basin plays an important role in flooding by delaying or accelerating surface flow. In the study area, the main LULC types are forest, farmland, grassland, shrubland, and settlement areas. About 2277.20 km² (40.69%) of the total LULC is covered by forest, followed by grassland
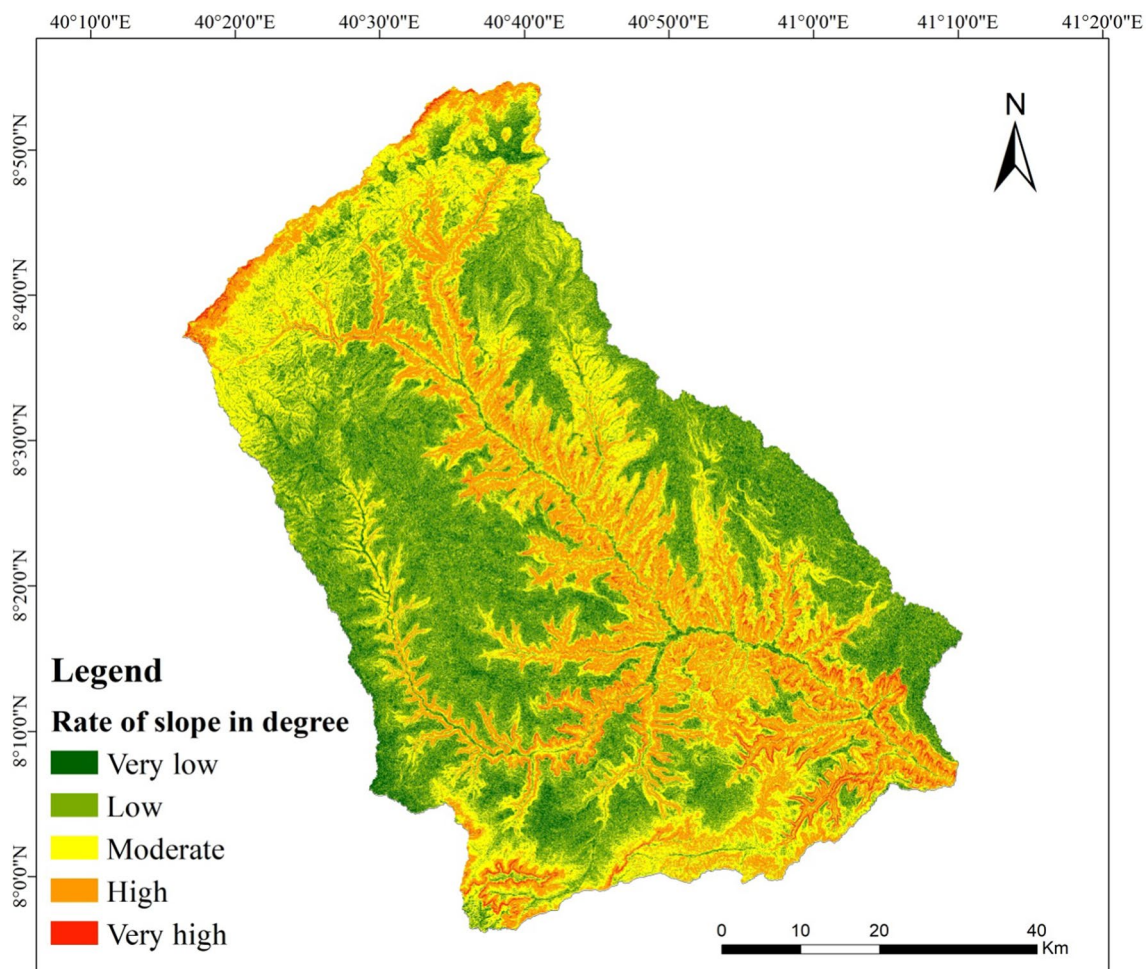

Fig. 4 Rate of slope for susceptibility to flooding

and farmland, which take up about 1460.08 km^2 (26.09%) and 1184.15 km^2 (21.16%), respectively (Table 8). From LULC types, farmland, settlement, grassland, shrubland, and forest were very high, high, moderate, low, and very low for flood risk in the study area, respectively. Spatially, the central and western parts of the study area were at higher risk for flooding than the northern and southern parts of the study area (Fig. 5). The result is more consistent with the previous study (Ayenew and Kebede 2023) that agriculture is more

Table 8 Land-use and land-cover factors

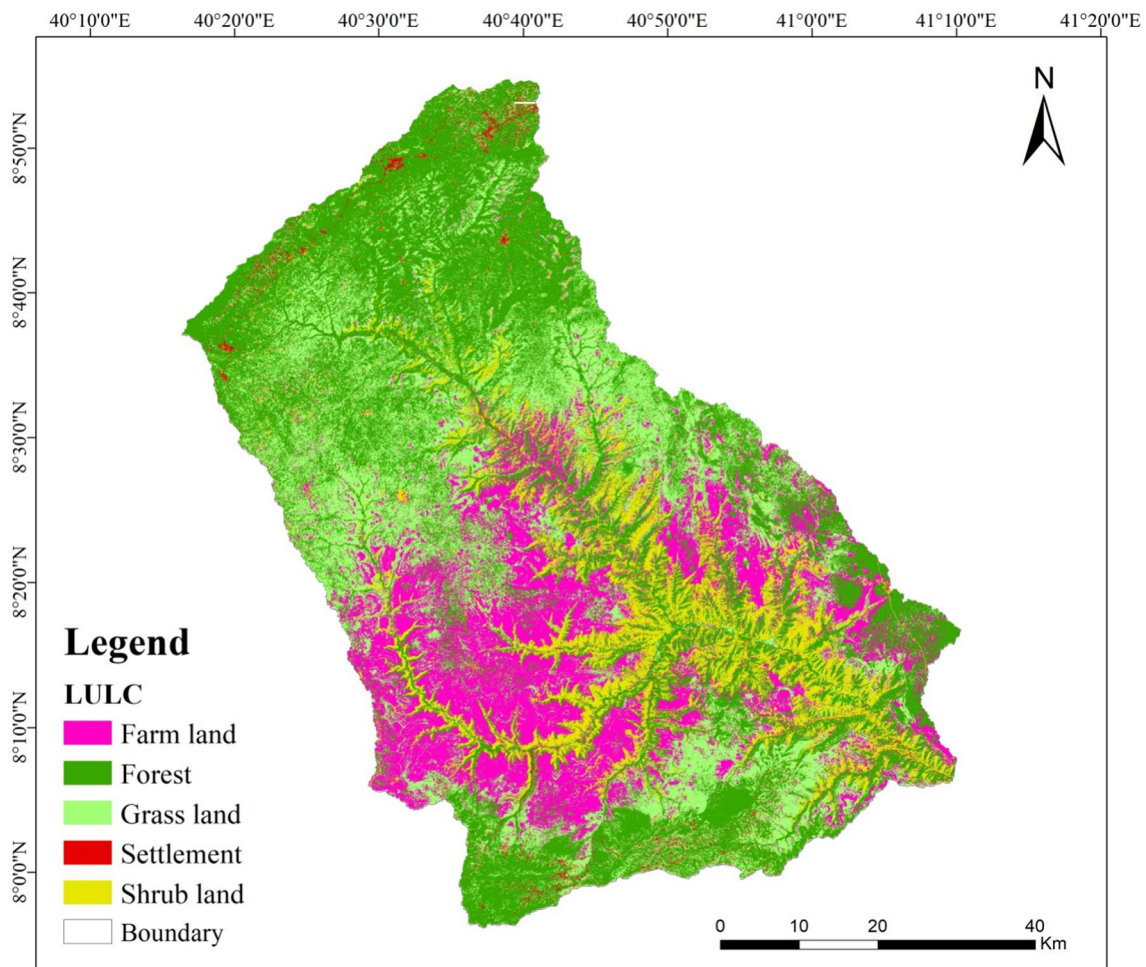| Class name	Area (km^2)	Area (%)
Shrubland	63.68	1.14
Settlement	611.23	10.92
Grassland	1460.08	26.09
Forest	2277.20	40.69
Farmland	1184.15	21.16
Total	5596.34	100

vulnerable than forest for flood risk in the case of the Dikala Watershed in Kobo Woreda, Amhara Region, Ethiopia.

Distance from rivers

Discharge increases as more water enters the stream through rainfall, tributary streams, or groundwater seeping in. Generally, as discharge rises, the stream's width, depth, and velocity all increase (Kiersh 1964). Any undeveloped low-lying land close to a river, lagoon, or lake is more vulnerable to flooding as the water level rises. Therefore, the risk of flooding decreases as the distance from the river increases, and flooding increases when the distance *is closer* to the river (Fig. 6). The river density of the study area was high and susceptible to flood inundation in the Wabi Shebele Sub-basin. The central and southern parts of the study area were at higher risk of flooding than the northern part of the Wabi Shebele Sub-basin. Negese et al. (2022) stated that flood inundation increased as the distance to the rivers decreased in the Dega Damot district, northwestern Ethiopia.

Fig. 5 Land-use/land-cover map

Fig. 6 Distance from rivers
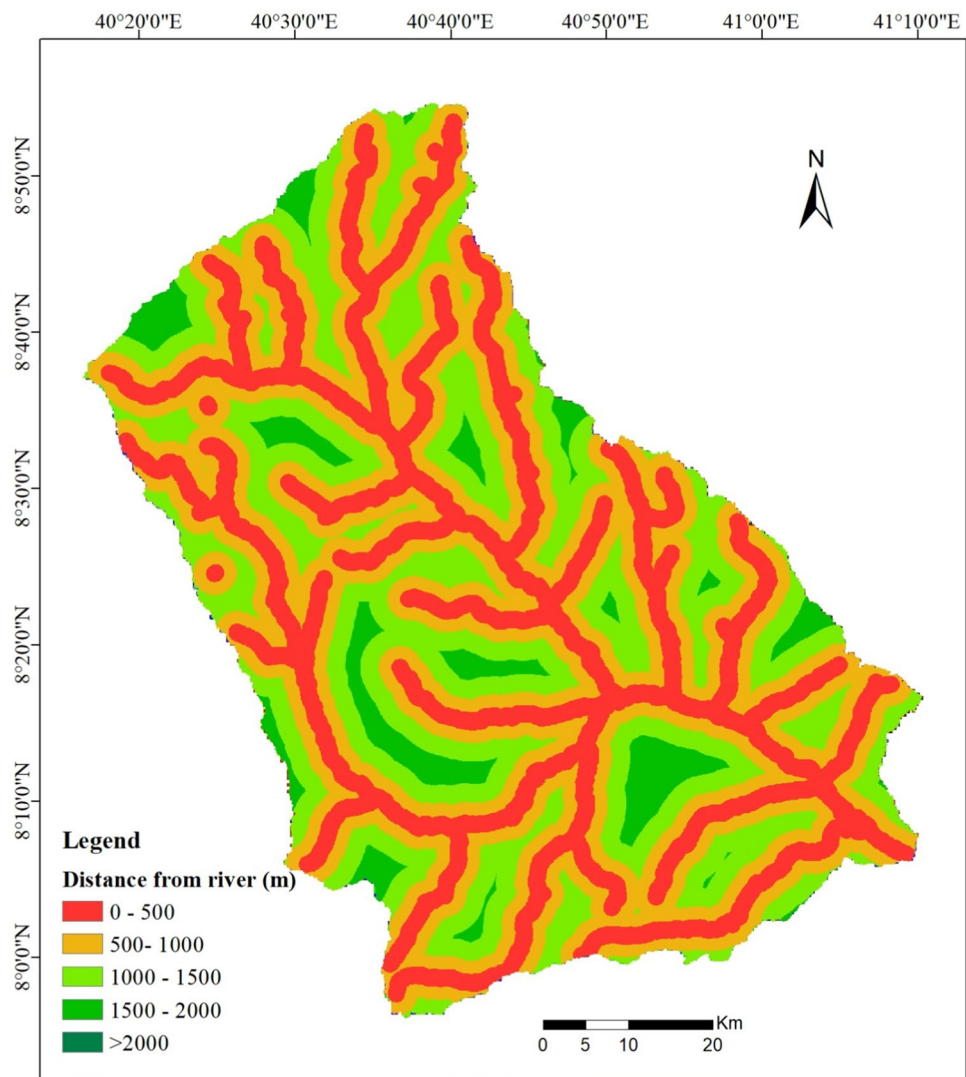
Rainfall factor

The massive groundwater system's primary source of recharge is rainfall on the highlands during the rainy season (Chen et al. 2023a). The area dominated by high rainfall was more vulnerable than the area captured with low rainfall for flooding in the Wabi *S*hebele Sub-basin. The regions with the highest recharge rates are the northwest, southeastern highlands, and upper basin. These aquifers are refilled by the streams that rise in the eastern highlands. Seasonal flooding occurs in the highlands during the summer, and the fragmented volcanic cover is favorable for groundwater recharge (Fig. 7). The amount, duration, and spatial distribution of rainfall in catchments are some of the most important factors influencing the risk of flooding (Assefa 2018; Chen et al. 2023b).

Elevation factor

Elevation was the main parameter used to assess the flood inundation of the study area. As a result, the area with moderate to low elevations was highly susceptible to flooding, whereas the area with high elevations was less vulnerable to flooding in the Wabi *S*hebele Sub-basin. In this study area, the upper and intermediate catchments (i.e., the northern and northwest parts of the sub-basin) have high elevation and experience low levels of flooding (Fig. 8). The central and southern parts of the study area were at high risk for flooding. However, the northern part of the study area was at low risk for flooding. The previous studies (Wondim 2016; Choubin et al. 2019; Ogato et al. 2020; Yin et al. 2023e) confirmed that low elevation was highly vulnerable *to* flooding and vice versa.
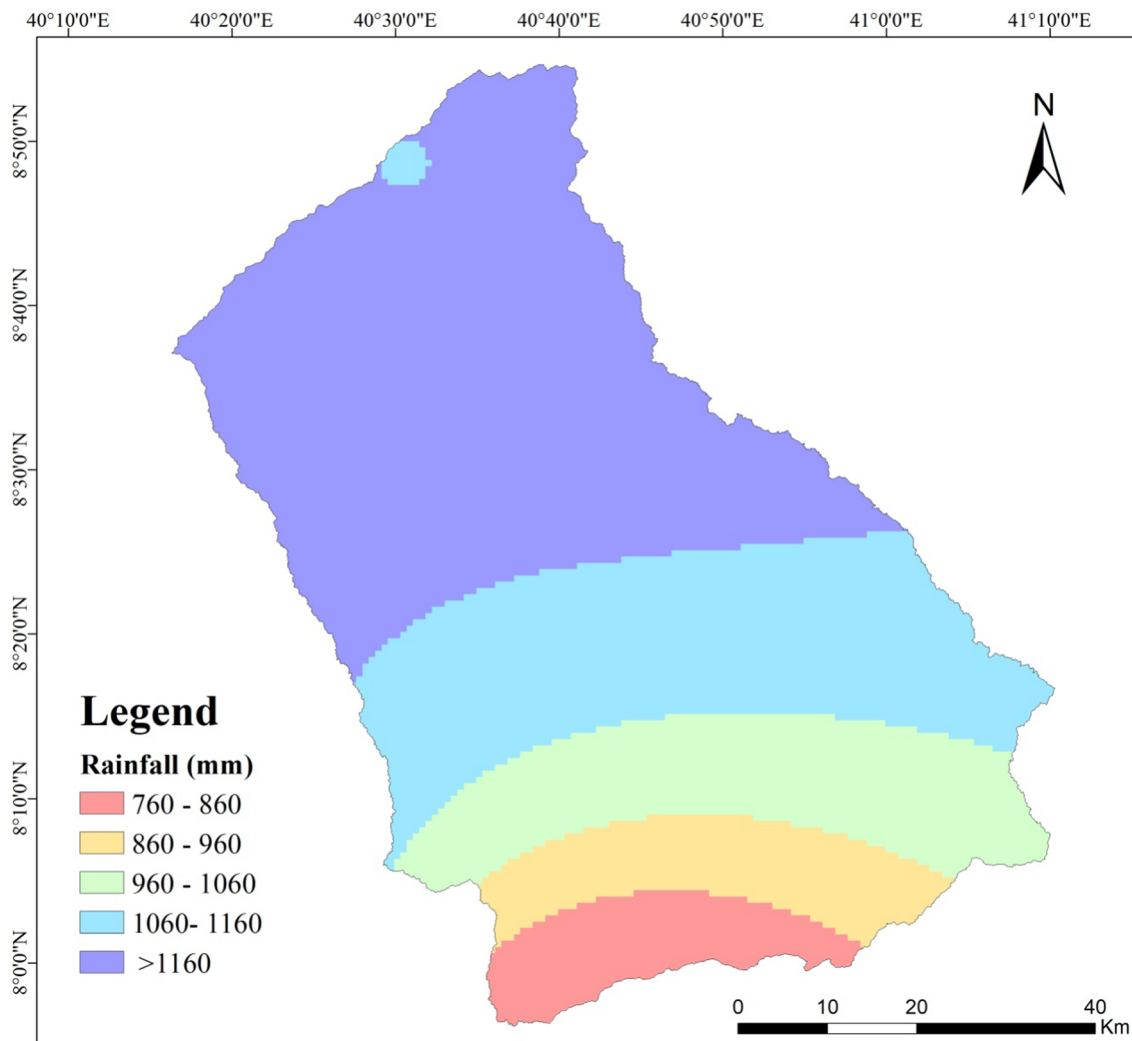
Fig. 7 Rainfall distribution map

Accuracy assessment

Overall accuracy assessment and kappa coefficients of the LULC types of 2022 were 92.5% and 0.89, respectively, in Wabi Shebele Sub-basin.

Potential flood risk map of the Wabi Shebele Sub-basin

Based on the significance of the elements and classes in the case study, weight and rank values were assigned to them. The element with the highest weight, according to expert knowledge and AHP results, was elevation (0.2899), followed by distance from rivers (0.2119), slope (0.1688), land use/land cover (0.1419), soil type (0.0849), and rainfall factor (0.1025) (Table 9). The resulting map was given a value corresponding to each pixel's factor and normalized weight after total scores were used to weight factors and rank classes.

According to the flood risk map (Fig. 9), the study area was subjected to have very high 527.31 km^2 (9.42%), high 2133.66 km^2 (38.12%), moderate 1906.44 km^2 (34.06%), low 847.35 km^2 (15.14%), and very low 182.54 km^2 (3.26%) flood risk, respectively (Table 8).

The levels of danger for the elements at risk in this study area are different. The worst-affected districts of the sub-basin are *Daro Labu,* with *a* very high flood risk 160.6 km^2 (14.7%) and *Hawi Gudina* district, with 284.78 km^2 (13.1%) (Table 10). The sub-districts of the study area are subject to varying degrees of flood risk. This difference is primarily the result of various environmental characteristics. The results of this study suggest that areas with a high concentration of farms and bare land, as well as low elevations, are at risk of flooding. Due to all of these factors, Woredas such as Daro Lebu, Burka Dintu, and Hawi Gudina are at high
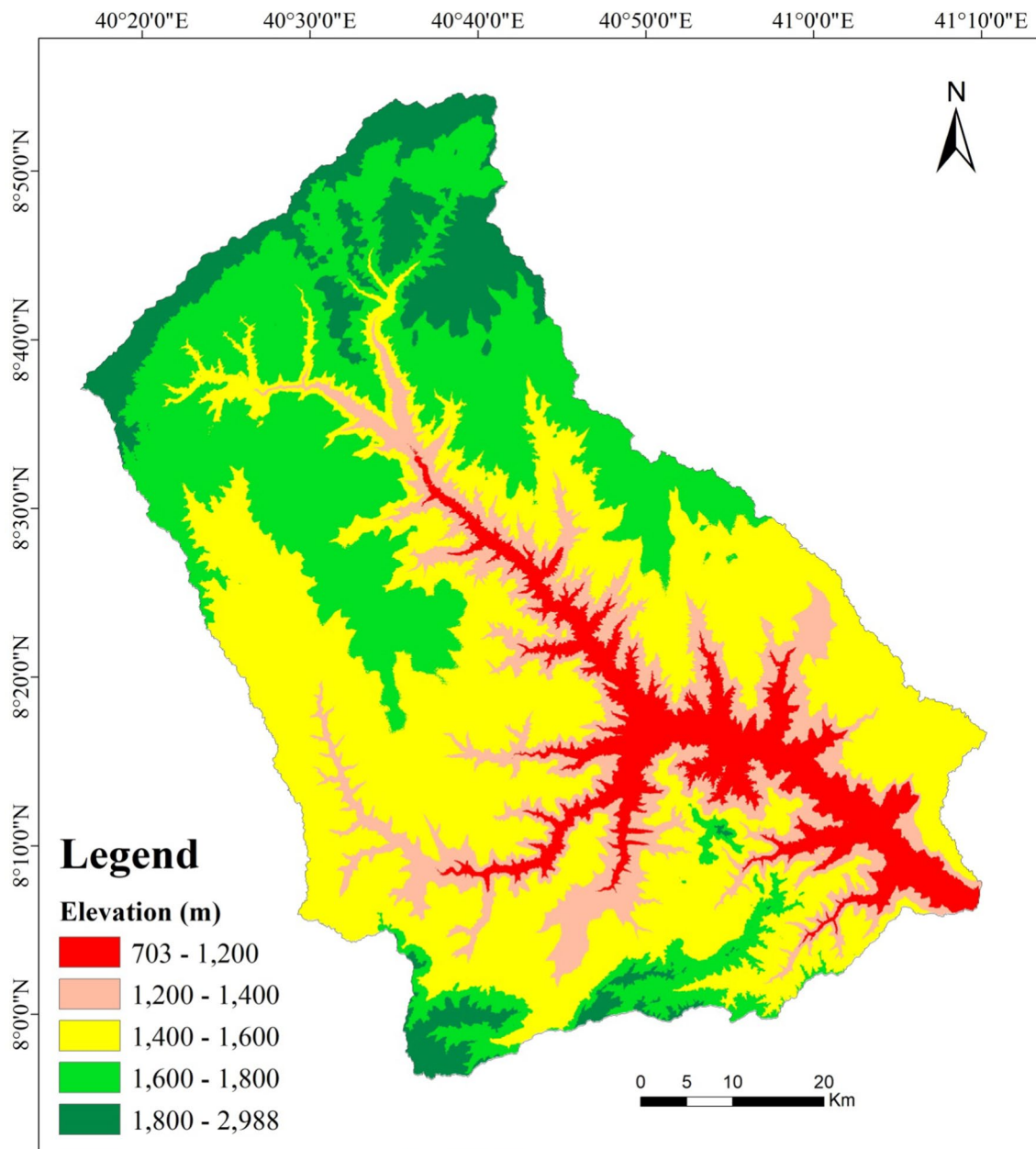
Fig. 8 Elevation map

Table 9 Level of flood risk

Level of flood risk	Area (km^2)	Area (%)
Very low	182.54	3.26
Low	847.35	15.14
Moderate	1906.44	34.06
High	2133.66	38.12
Very high	527.31	9.42

risk of flooding. This finding supports Assefa (2018) and Hagos et al. (2022) who found that factors such as unpredictable drainage areas, rapidly changing topography, and low ground surface infiltration capacity all increase flood risk. While flooding occurs frequently in nature, human land-use activities typically involve destroying natural vegetation (for farming or construction), which can significantly increase runoff and raise the risk of flash floods and river floods.
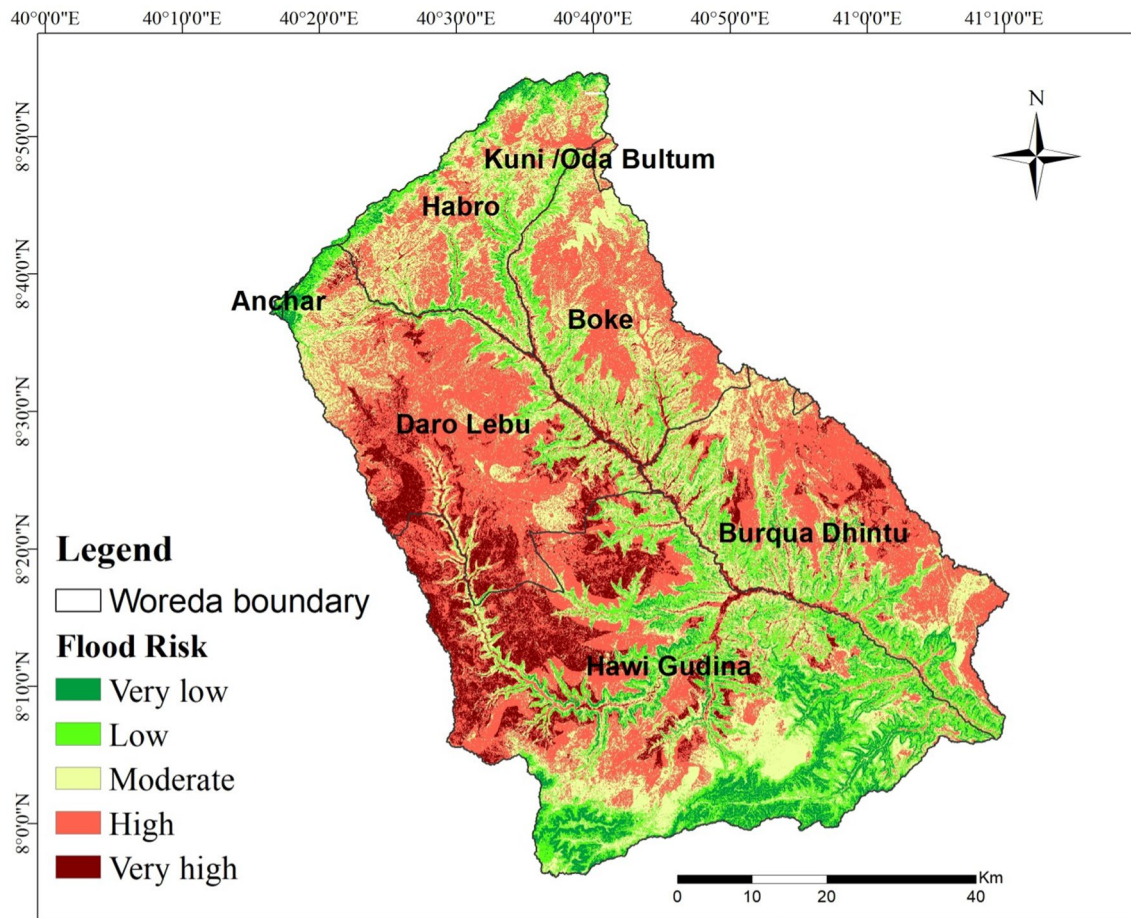
Fig. 9 Flood risk map

Table 10 Districts of the sub-basin

Districts in the sub-basin	Area (km^2)	Percentage share (%)
Habro	627.68	11.22
Daro Lebu	1096.98	19.62
Boke	672.84	12.03
Kuni/Oda Bultum	17.92	0.32
Hawi Gudina	2175.46	38.90
Burka Dintu	1004.51	17.96

Conclusion

Assessment of flood risk is an important strategic planning tool for monitoring flood risk. This study investigated flood risk areas *using* geospatial techniques in *the* Wabi Shebele River Sub-basin of Southeast Ethiopia. The dataset*s* used in the study include Landsat OLI/TIRS of 2022, soil types, climate (rainfall), and topographic data (*s*lope and elevation).

The collected data were analyzed by integrati*ng* geospatial techniques with *an* analytic hierarchy process for generating *a* flood risk map in the study area. Environmental factors such as soil type, slope, elevation, rainfall, and distance from rivers, as well as land-cover types, were the essential parameters for assessing flood risk *in the* Wabi *S*hebele Sub-basin.

The result revealed that about 9.42, 38.12, 34.06, and 15.14% of the total area are at risk of flooding, with very high, high, moderate, and low flood risk, respectively. This result indicates that the study area was extremely susceptible to flood risk due to topographic variation and the expansion of agricultural land in low and high land areas, which aggravates the rate of deforestation and surface runoff. As a result, within the six districts in the study area, four districts were in very high flood risk classes. Identification of the flood risk-prone area was essential for prioritizing future management strategies in the study area. Based on this study, we recommended that environmental and climate change resilience specialists, natural resource managers, and any other concerned bodies assume crucial responsibility for appropriate flood control strategies in the study area.

Declarations

Conflict of interest The authors declared that there is no conflict of interest.

Consent for publication The authors agreed to publish in journal of applied water science.

References

Abaya SW, Mandere N, Ewald G (2009) Floods and health in Gambella region, Ethiopia: a qualitative assessment of the strengths and weaknesses of coping mechanisms. Glob Health Action 2:1–10

Assefa T (2018) Flood risk assessment in Ethiopia. Civ Environ Res 10:35–40

Ayenew WA, Kebede HA (2023) GIS and remote sensing based flood risk assessment and mapping: the case of Dikala Watershed in Kobo Woreda Amhara region, Ethiopia. Environ Sustain Indic 18:100243

Bhatt B (2008) Remote sensing and GIS. Oxford University Press, Oxford

Chen J, Liu Z, Yin Z, Liu X, Li X, Yin L, Zheng W (2023a) Predict the effect of meteorological factors on haze using BP neural network. Urban Clim 51:101630. https://doi.org/10.1016/j.uclim.2023.101630

Chen W, Liu W, Liang H, Jiang M, Dai Z (2023b) Response of storm surge and M2 tide to typhoon speeds along coastal Zhejiang Province. Ocean Eng 270:113646. https://doi.org/10.1016/j.oceaneng.2023.113646

Choubin B, Moradi E, Golshan M, Adamowski J, Sajedi-Hosseini F, Mosavi A (2019) An ensemble prediction of food susceptibility using multivariate discriminant analysis, classifcation and regression trees, and support vector machines. Sci Total Environ 651:2087–2096

Gao C, Zhang B, Shao S, Hao M, Zhang Y, Xu Y, Wang Z (2023) Risk assessment and zoning of flood disaster in Wuchengxiyu Region, China. Urban Clim 49:101562. https://doi.org/10.1016/j.uclim.2023.101562

Getahun YS, Gebre SL (2015) Flood hazard assessment and mapping of flood inundation area of the Awash River Basin in Ethiopia using GIS and HEC-GEORAS/HEC-RAS model. J Civ Environ Eng 5(4):1–12

Girma R, Gebre E, Tadesse T (2020) Land suitability evaluation for surface irrigation using spatial information technology in Omo-Gibe River Basin, Southern Ethiopia. Irrigat Drainage Syst Eng 9(2)

Hagos YG, Andualem TG, Yibeltal M, Mengie MA (2022) Flood hazard assessment and mapping using GIS integrated with multi-criteria decision analysis in upper Awash River basin, Ethiopia

Huang S, Huang M, Lyu Y (2021) Seismic performance analysis of a wind turbine with a monopile foundation affected by sea ice based on a simple numerical method. Eng Appl Comput Fluid Mech 15(1):1113–1133. https://doi.org/10.1080/19942060.2021.1939790

Kundzewicz ZW, Stoffel M (2016) Flood risk in the Upper Vistula Basin. Springer, Cham, pp 39–52. https://doi.org/10.1007/978-3-319-41923-7

Li W, Zhu J, Fu L, Zhu Q, Xie Y, Hu Y (2021) An augmented representation method of debris flow scenes to improve public perception. Int J Geogr Inf Sci 35(8):1521–1544. https://doi.org/10.1080/13658816.2020.1833016

Li Q, Song D, Yuan C, Nie W (2022) An image recognition method for the deformation area of open-pit rock slopes under variable rainfall. Measurement 188:110544. https://doi.org/10.1016/j.measurement.2021.110544

Liu YS, Yuan XM, Guo L, Huang YH, Zhang XL (2017) Driving force analysis of the temporal and spatial distribution of flash floods in Sichuan Province. Sustainability. https://doi.org/10.3390/su9090152

Lyu HM, Shen SL, Zhou A, Yang J (2019) Perspectives for flood risk assessment and management for mega-city metro system. Tunn Undergr Space Technol 84:31–44

Ma S, Qiu H, Yang D, Wang J, Zhu Y, Tang B, Cao M (2023) Surface multi-hazard effect of underground coal mining. Landslides 20(1):39–52. https://doi.org/10.1007/s10346-022-01961-0

Merga BB, Moisa MB, Negash DA, Ahmed Z, Gemeda DO (2022) Land surface temperature variation in response to landuse and land-cover dynamics: a case of Didessa River sub-basin in western Ethiopia. Earth Syst Environ. https://doi.org/10.1007/s41748-022-00303-3

Miller HJ, Shaw SL (2015) Geographic information systems for transportation in the 21st century. Geogr Compass 9:180–189

Ministry of Water Resources (MoWR) (2004) Wabi Shebele River Basin Integrated Master Plan Study Project, Water Resources, Part 2: Hydrology, Land Use/Cover Study

Moisa MB, Gemeda DO (2021) Analysis of urban expansion and land use/land cover changes using geospatial techniques: a case of Addis Ababa City, Ethiopia. Appl Geomat 13:853–861

Moisa MB, Dejene IN, Merga BB, Gemeda DO (2022) Impacts of land use/land cover dynamics on land surface temperature using geospatial techniques in Anger River Sub-basin, Western Ethiopia. Environ Earth Sci 81(3):1–14

Negash DA, Moisa MB, Merga BB, Sedeta F, Gemeda DO (2021) Soil erosion risk assessment for prioritization of sub-watershed: the case of Chogo Watershed, Horo Guduru Wollega, Ethiopia. Environ Earth Sci 80:589. https://doi.org/10.1007/s12665-021-09901-2

Negese A, Worku D, Shitaye A, Getnet H (2022) Potential flood-prone area identification and mapping using GIS-based multi-criteria decision-making and analytical hierarchy process in Dega Damot district, northwestern Ethiopia. Appl Water Sci 12(12):255

Ogato GS, Bantider A, Abebe K, Geneletti D (2020) Geographic information system (GIS)—based multi criteria analysis of fooding

hazard and risk in Ambo Town and its watershed, West shoa zone, Oromia regional State Ethiopia. J Hydrol Reg Stud. https://doi.org/10.1016/j.ejrh.2019.10

Saaty TL (1980) The analytic hierarchy process. McGraw-Hill, New York

Saaty TL (2008) Decision making with the analytic hierarchy process. Int J Serv Sci 1:83–98

Sun R, Gong Z, Gao G, Shah AA (2020) Comparative analysis of multi-criteria decision-making methods for flood disaster risk in the Yangtze River Delta. Int J Disaster Risk Reduct 51:101768

Ullah K, Zhang J (2020) GIS-based flood hazard mapping using relative frequency ratio method: a case study of Panjkora River Basin, eastern Hindu Kush, Pakistan. PLoS ONE 15(3):e0229153

Wondim YK (2016) Flood hazard and risk assessment using GIS and remote sensing in lower Awash sub-basin Ethiopia. J Environ Earth Sci 6(9):69–86

Wu B, Quan Q, Yang S, Dong Y (2023) A social-ecological coupling model for evaluating the human-water relationship in basins within the Budyko framework. J Hydrol 619:129361. https://doi.org/10.1016/j.jhydrol.2023.129361

Xie X, Xie B, Cheng J, Chu Q, Dooling T (2021) A simple Monte Carlo method for estimating the chance of a cyclone impact. Nat Hazards 107(3):2573–2582. https://doi.org/10.1007/s11069-021-04505-2

Xu Z, Wang Y, Jiang S, Fang C, Liu L, Wu K, Chen Y (2022) Impact of input, preservation and dilution on organic matter enrichment in lacustrine rift basin: a case study of lacustrine shale in Dehui Depression of Songliao Basin, NE China. Mar Petroleum Geol 135:105386. https://doi.org/10.1016/j.marpetgeo.2021.105386

Yang D, Qiu H, Ye B, Liu Y, Zhang J, Zhu Y (2023) Distribution and recurrence of warming-induced retrogressive thaw slumps on the Central Qinghai-Tibet Plateau. J Geophys Res Earth Surf. https://doi.org/10.1029/2022JF007047

Yin H, Wu Q, Yin S, Dong S, Dai Z, Soltanian MR (2023a) Predicting mine water inrush accidents based on water level anomalies of borehole groups using long short-term memory and isolation forest. J Hydrol 616:128813. https://doi.org/10.1016/j.jhydrol.2022.128813

Yin H, Zhang G, Wu Q, Yin S, Soltanian MR, Thanh HV, Dai Z (2023b) A deep learning-based data-driven approach for predicting mining water inrush from coal seam floor using microseismic monitoring data. IEEE Trans Geosci Remote Sens. https://doi.org/10.1109/TGRS.2023.3300012

Yin L, Wang L, Ge L, Tian J, Yin Z, Liu M, Zheng W (2023c) Study on the thermospheric density distribution pattern during geomagnetic activity. Appl Sci. https://doi.org/10.3390/app13095564

Yin L, Wang L, Keim BD, Konsoer K, Yin Z, Liu M, Zheng W (2023d) Spatial and wavelet analysis of precipitation and river discharge during operation of the Three Gorges Dam, China. Ecol Indic 154:110837. https://doi.org/10.1016/j.ecolind.2023.110837

Yin L, Wang L, Li T, Lu S, Yin Z, Liu X, Zheng W (2023e) U-Net-STN: a novel end-to-end lake boundary prediction model. Land 12(8):1602. https://doi.org/10.3390/land12081602

Yin Z, Liu Z, Liu X, Zheng W, Yin L (2023f) Urban heat islands and their effects on thermal comfort in the US: New York and New Jersey. Ecol Ind 154:110765. https://doi.org/10.1016/j.ecolind.2023.110765

Yuan C, Li Q, Nie W, Ye C (2023) A depth information-based method to enhance rainfall-induced landslide deformation area identification. Measurement 219:113288. https://doi.org/10.1016/j.measurement.2023.113288

Zhang JY, Chen YB (2019) Risk assessment of flood disaster induced by typhoon rainstorms in Guangdong Province. China Sustainability 11:2738

Zhao Z, Xu G, Zhang N, Zhang Q (2022) Performance analysis of the hybrid satellite-terrestrial relay network with opportunistic scheduling over generalized fading channels. IEEE Trans Veh Technol 71(3):2914–2924. https://doi.org/10.1109/TVT.2021.3139885

Zhou G, Deng R, Zhou X, Long S, Li W, Lin G, Li X (2021a) Gaussian inflection point selection for LiDAR hidden echo signal decomposition. IEEE Geosci Remote Sens Lett 19:1–5. https://doi.org/10.1109/LGRS.2021.3107438

Zhou G, Li W, Zhou X, Tan Y, Lin G, Li X, Deng R (2021b) An innovative echo detection system with STM32 gated and PMT adjustable gain for airborne LiDAR. Int J Remote Sens 42(24):9187–9211. https://doi.org/10.1080/01431161.2021.1975844

Zhu W, Chen J, Sun Q, Li Z, Tan W, Wei Y (2022) Reconstructing of high-spatial-resolution three-dimensional electron density by ingesting SAR-derived VTEC into IRI model. IEEE Geosci Remote Sens Lett. https://doi.org/10.1109/LGRS.2022.3178242